

Inhibitors of multidrug resistance (MDR) have affinity for MDR substrates

Mire Zloh,^{a,*} Glenn W. Kaatz^b and Simon Gibbons^{c,*}

^a*Department of Pharmaceutical and Biological Chemistry, The School of Pharmacy, University of London, 29–39 Brunswick Square, London WC1N 1AX, UK*

^b*Division of Infectious Diseases, Department of Internal Medicine, School of Medicine, Wayne State University and the John D. Dingell Department of Veterans Affairs Medical Center, Detroit, MI 48201, USA*

^c*Centre for Pharmacognosy and Phytotherapy, The School of Pharmacy, University of London, 29–39 Brunswick Square, London WC1N 1AX, UK*

Received 16 September 2003; revised 12 November 2003; accepted 3 December 2003

Abstract—Multidrug-resistance (MDR) occurs in many bacterial species and tumour cells. MDR functions by membrane proteins which export drugs from cells, resulting in a low ineffective concentration of the drug. We have shown by molecular modelling that inhibitors of MDR have affinity for substrates of MDR transporters. This affinity may facilitate drug entry into cells and a large inhibitor–drug complex may be a poorer substrate for the MDR mechanism. This complex would effectively ‘cloak’ the drug rendering it unavailable for efflux.

© 2003 Elsevier Ltd. All rights reserved.

Multidrug-resistance (MDR) occurs in many bacteria, fungi and tumour cells¹ and this phenomenon is responsible for exporting drugs from cells, resulting in a low ineffective concentration of the drug.² A common feature of MDR mechanisms is their ability to recognise many structurally unrelated substrates³ and remove them from the cell, and inhibitors of these transport processes are thought to act by directly binding to hydrophobic regions of MDR proteins causing inhibition of xenobiotic removal.⁴ A number of these transporters have been characterised for mammalian cells including *p*-glycoprotein (*p*-gp)² and multidrug resistance related protein (MRP),⁵ both of which confer resistance to cytotoxic agents. In Gram-positive and Gram-negative bacteria, MDR pumps such as NorA⁶ (*Staphylococcus aureus*) and MexAB-OprM⁷ (*Pseudomonas aeruginosa*) export a wide array of antiseptics and antibiotics including fluoroquinolones.

It is not known exactly how inhibitors of MDR transporters function but there are a few proposed mechanisms of action: direct binding of inhibitor to one or

more binding sites on the protein therefore blocking transport as either competitive or non-competitive inhibitors,² depletion of pump energy by inhibiting binding of ATP and modifying protein conformation by an inhibitor interaction with the cell membrane.⁸ There is indirect evidence by Ahmed et al.,⁹ that reserpine does bind to a hydrophobic region of the Bmr MDR transporter of *Bacillus subtilis* causing inhibition of efflux.

It seemed possible to us that inhibitors of MDR may have an affinity for substrates and bind them to form a complex which may facilitate entry of the drug into the cell and also importantly from the perspective of MDR inhibition, this complex may not be recognised by the transporter. In the cell this complex could then dissociate to release inhibitor and drug. To investigate our hypothesis, we conducted a series of molecular modelling experiments to study the affinity that inhibitors of MDR phenomena have with MDR substrates.

The modelling work presented here was performed using ChemOffice 2002,¹⁰ GRID 20,¹¹ Molden,¹² and Viewer Lite 5.0¹³ software packages. In order to model the MDR inhibitors, antibiotics and anticancer drugs, molecular mechanical and semi-empirical theory were used. The structures of each molecule were initially drawn by ChemDraw. Each 2D structure was converted

Keywords: MDR; Multidrug-resistance; Molecular modelling; Mechanism; Bacteria; Tumour.

* Corresponding authors. Tel.: +44-20-7753-5879; fax: +44-20-7753-5964; (M.Z.); tel.: +44-20-7753-5913, fax: +44-20-7753-5909 (S.G.); e-mail: mire.zloh@ulsop.ac.uk; simon.gibbons@uslop.ac.uk

into 3D structure by Chem3D, followed by molecular mechanics minimization using MM2 force field. MM2 parameters used here are from the full MM2 Parameter Set including π -systems, as provided by N. L. Allinger and implemented in Chem3D.¹⁰

The resulting structures were further subjected to altered simulated annealing protocol consisting of 4 ps molecular dynamics at 300 K to explore conformational space. Five visibly different structures (not necessarily lowest energy conformations) for each molecule were chosen from the trajectory and subjected to 2 ps molecular dynamics at 100 K. The last structure in the trajectory was minimized using MM2 energy minimization and further optimized using MOPAC 2000 and the AM1 method. MM2 and Mopac 2000 were implemented in the Chem3D software. Semi-empirical AM1 geometries of MDR inhibitors and drugs were used as input files for GRID 20 software. The whole molecule was considered during calculations and all GRID parameters were kept at their default values. Inhibitor molecules were chosen to be target molecules during calculations, since those were generally larger than drug molecules. All interactions were examined by using GROUP probes implemented in GRID software representing relevant functional groups of drug molecules. All reported interaction energies were predicted using GRID20 software.

This study was conducted on inhibitors of *p*-glycoprotein mediated MDR and between cytotoxic drugs which are substrates of this mechanism (Table 1). Additionally, inhibitors of bacterial MDR in combination with fluoroquinolone antibiotics, some of which are substrates for the bacterial MDR efflux systems NorA and MexAB–OprM, were also studied (Table 1). We have examined pairs of MDR inhibitor–drug (substrate) which have experimental data showing that the inhibitor restores activity of the drug.^{14–24}

For inhibitors which showed reversal of MDR, the energy of interaction of the drug with corresponding inhibitor was calculated by GRID 20 software as negative and greater than -10 kcal/mol, which indicated that it was highly likely that these pairs have the ability to form a complex. Table 1 shows the energy of interaction for a wide range of MDR inhibitor–drug complexes and to highlight these findings, below we discuss selected examples from the anticancer and antibacterial fields of MDR.

Specifically, the anticancer drugs doxorubicin and vinblastine were shown to bind to reserpine (Fig. 1a and b) at the same moiety of the reserpine molecule, notably the A, B and C-rings, although the mode of binding of these two drugs to reserpine is different. In the case of doxorubicin, an interaction was observed between its aromatic rings and those of the inhibitor, whilst in the case of the vinblastine–reserpine complex, the aromatic region of reserpine fitted into the curvature of the vinblastine molecule (Fig. 1b) being perpendicular to the aromatic rings of vinblastine. In both cases the energy of interactions are comparable.

For the inhibitor GG918, four combinations with the cytotoxic drugs doxorubicin, topotecan, mitoxantrone and vinblastine were studied. For all of these complexes, the cytotoxic drug bound to the middle portion of GG918, which links the acridone and isoquinoline moieties, and the interaction appears to be non-specific, with topotecan (Fig. 1c) having the highest energy of interaction (Table 1). Drug–inhibitor complex pairs represented here have the highest energy of interaction and it must be noted that a range of other complex conformations were detected. Although the position of the drug with respect to inhibitor is different, most significantly, the same part of the inhibitor is involved in all complexes, even with different drugs.

This non-specificity of interaction possibly enables the MDR inhibitor to recognise and bind a wide array of structurally unrelated drugs and to restore their efficacy.

α -Tocopherol, which has been shown to reverse the effects of MDR inhibitors,¹⁶ has a higher energy of interaction with MDR inhibitors than substrates (-19.06 kcal/mol with GG918). Furthermore, it binds to the same portion of the inhibitor as the substrates (Fig. 1d) suggesting that it may function by preferentially binding to the inhibitor and therefore preventing the formation of an inhibitor–drug complex.

Four inhibitors of bacterial MDR were chosen with fluoroquinolones as efflux substrates. Two of these, reserpine and GG918 have been shown to be inhibitors of Gram-positive MDR transporters such as the *S. aureus* NorA system.¹⁷ The last two, MC-002,595 and MC-207,110 are inhibitors of the MexAB–OprM and AcrAB–TolC MDR efflux mechanisms found in Gram-negative species.¹⁸

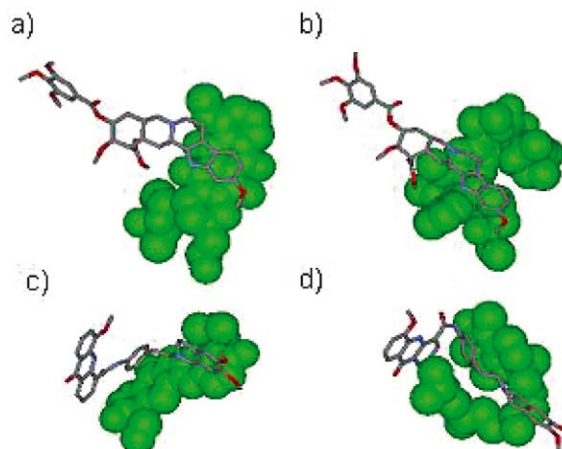


Figure 1. Highest interaction energy complexes between MDR inhibitors and ligand molecules (ligand molecules are represented in green): (a) binding between A, B and C rings of reserpine and doxorubicin, indicating π – π stacking between aromatic moieties of the two molecules; (b) reserpine and vinblastine interaction depicting the aromatic region of reserpine fitting into the curvature of the vinblastine molecule. The A, B and C rings of reserpine are perpendicular to the aromatic rings of vinblastine; (c) GG918 and topotecan complex; (d) GG918 and α -tocopherol complex depicting the position of the ligand molecule binding strongly to the binding site for substrates.

In all cases of the reserpine–fluoroquinolone anti-microbial agent complexes, the binding site is the same for that as the anticancer drugs, being binding to the first three rings of the reserpine structure as demonstrated in Figure 2a for the norfloxacin–reserpine

complex. Again all energies of interaction were comparable, although modes of binding were not the same. For GG918, the binding site of the fluoroquinolones to the inhibitor is also the same region as that for the anticancer drugs as represented in Figure 2b

Table 1. Interaction energies between different drugs and MDR inhibitors calculated by GRID 20 software in correlation with the reported MDR inhibition

Drug	MDR Inhibitor	Inhibition	Interaction energy (kcal/mol)
Doxorubicin	Reserpine	2.9 ^{a,14}	−12.01
Vinblastine	Reserpine	8.0 ^{a,14}	−11.63
Mitoxantrone	GG918	1.2–1850 ^{b,15}	−13.02
Topotecan	GG918	1.0–23 ^{b,15}	−16.15
Doxorubicin	GG918	~58% reduction ^{c,16}	−13.42
Vinblastine	GG918	~95% reduction ^{c,16}	−15.89
α-Tocopherol	GG918	Reversal of MDR inhibition ¹⁶	−19.06
Norfloxacin	Reserpine	4 ^{d,17}	−13.29
Ciprofloxacin	Reserpine	8 ^{d,17}	−12.94
Levofloxacin	Reserpine	2 ^{d,17}	−13.32
Moxifloxacin	Reserpine	2 ^{d,17}	−12.95
Norfloxacin	GG918	8 ^{d,17}	−13.57
Ciprofloxacin	GG918	8 ^{d,17}	−13.94
Levofloxacin	GG918	2 ^{d,17}	−15.24
Moxifloxacin	GG918	0 ^{d,17}	−14.58
NPN	MC-002,595	2.3 ^{e,18}	−12.97
Levofloxacin	MC-207,110	2–64 ^{f,18}	−13.75
Vincristine	JTV-519	3.7 ^{g,19}	−15.05
Taxol	JTV-519	24.8 ^{g,19}	−13.18
Etoposide (VP-16)	JTV-519	2.6 ^{g,19}	−13.18
Doxorubicin	JTV-519	2.7 ^{g,19}	−15.59
Actinomycin D	JTV-519	3 ^{g,19}	−12.15
STI571	JTV-519	3.1 ^{g,19}	−13.10
Taxol	VX-710	Successful in clinical trial ²⁰	−10.64
Daunorubicin	XR-9576	IC ₅₀ = 38.18 nM ²¹	−14.98
Vincristine	Sinensetin	72.28 ^{h,22}	−10.1
Doxorubicin	Indomethacin	0.251/NA ^{i,23}	−18.60
Doxorubicin	Sulindac	0.368/0.449 ^{i,23}	−15.23
Doxorubicin	Tolmetin	0.357/0.467 ^{i,23}	−13.05
Vincristine	Indomethacin	0.301/NA ^{i,23}	−16.66
Vincristine	Sulindac	0.462/0.241 ^{i,23}	−16.10
Vincristine	Tolmetin	NA/0.593 ^{i,23}	−15.73
Etoposide	Indomethacin	0.916/0.534 ^{i,23}	−15.50
Etoposide	Sulindac	0.681/0.463 ^{i,23}	−15.02
Etoposide	Tolmetin	NA/0.745 ^{i,23}	−12.58
Taxol	Indomethacin	2.234/1.227 ^{i,23}	−12.90
Taxol	Sulindac	1.539/1.233 ^{i,23}	−12.43
Taxol	Tolmetin	1.349/NA ^{i,23}	−9.18
Doxorubicin	Tetrandrine	5.4–20.4 ^{i,23}	−12.89
Doxorubicin	Verapamil	~33% reduction ^{c,16}	−12.73
Vinblastine	Verapamil	~88% reduction ^{c,16}	−12.53
α-Tocopherol	Verapamil	Reversal of inhibition ¹⁶	−15.39
Doxorubicin	Clofazimine	~40% reduction ^{c,16}	−23.70
Vinblastine	Clofazimine	~94% reduction ^{c,16}	−20.25
α-Tocopherol	Clofazimine	Reversal of inhibition ¹⁶	−29.55
Doxorubicin	B669	~31% reduction ^{c,16}	−20.59
Vinblastine	B669	~95% reduction ^{c,16}	−17.94
α-Tocopherol	B669	Reversal of inhibition ¹⁶	−20.80
Doxorubicin	α-Tocopherol	0% reduction ^{c,16}	−13.64
Vinblastine	α-Tocopherol	0% reduction ^{c,16}	−14.24
Norfloxacin	Agent from <i>Lycopodium europaeus</i>	No inhibitory activity ²⁵	−8.51

^a Fold increase, IC₅₀ for drug alone/IC₅₀ for drug in the presence of inhibitor.

^b DMF, dose modifying factor defines as the IC₅₀ for the chemotherapy drug without GG918 divide by IC₅₀ with GG918.

^c Approximate percentage for the level of inhibition of cell growth in the presence of cytotoxic drug in the presence and absence of inhibitor using H69/LX4 cells. This was calculated using the percentage growth value of inhibitor + drug divided by the value for drug.

^d Fold reduction in minimum inhibitory concentration (MIC) of antibiotic in the presence of inhibitor.

^e Fold reduction in fluorescence in presence of inhibitor (128 µg/mL) compared to absence of inhibitor.

^f Ratio between the MIC without efflux pump inhibitor (EPI) and the MIC in the presence of a potentiating concentration of EPI.

^g Relative resistance determined by dividing the IC₅₀ values of drugs with or without the inhibitors by that without the reversing agents.

^h Chemosensitizing index IC₅₀ (vincristine)/IC₅₀ (vincristine + inhibitor).

ⁱ Combination index (CI) values, a quantitative measure of drug interaction in terms of an additive (CI = 1), synergistic (CI < 1) or antagonistic (CI > 1) effect. Values quoted for two different cell lines (A549/DLKP). NA is not available.

^j Fold-reversal, ratio of the IC₅₀ for doxorubicin alone versus the IC₅₀ for doxorubicin in the presence of the modulating agent.

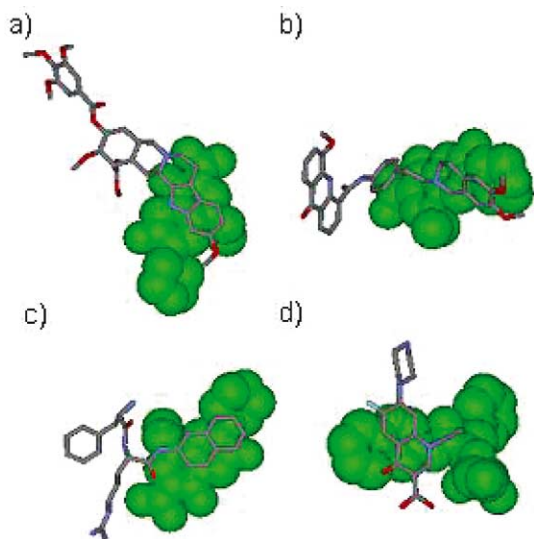


Figure 2. Highest interaction energy complexes between MDR inhibitors and substrates for bacterial MDR (substrate molecules are represented in green): (a) reserpine strongly binds norfloxacin at the same binding site for anticancer drugs, namely rings A, B and C; (b) binding site of GG918 for norfloxacin is the same as for the topotecan complex; (c) the aromatic moiety of the MC-207,110 strongly binds the antibiotic levofloxacin and (d) the interaction between MC-002,595 and NPN involves π - π stacking of the aromatic rings.

for the GG918-norfloxacin complex, and energies of interactions are given in Table 1. Interestingly, a recently isolated plant natural product from *Lycopus europaeus*,²⁵ which did not modulate the activity of norfloxacin and therefore is not an inhibitor of NorA in *S. aureus*, showed a low energy of interaction with norfloxacin (−8.51 kcal/mol). Whilst this compound possesses similar lipophilic properties to reserpine, it is a non-aromatic highly chiral non-planar compound, which may account for its low predicted interaction with aromatic planar achiral norfloxacin. This would again support the importance of complex formation between MDR inhibitor and drug for reversal of MDR.

The inhibitors of the MexAB–OprM and AcrAB–TolC MDR transporters, MC-207,110 and MC-002,595, have a similar binding site for all fluoroquinolones investigated, being the quinoline portion of the molecule. In Fig 2c and d, complexes between MC-207,110 and levofloxacin, and MC-002,595 and NPN (*N*-phenylnaphthylamine, a fluorescent substrate for the AcrAB–TolC mechanism), are shown. Interaction energies are within the range of 1 kcal/mol for both substrate–inhibitor complexes investigated. Again, as in the previous case, each inhibitor bound the substrate at the same site on the inhibitor but with a different portion of each substrate.

Interestingly, the Gram-positive bacterial MDR inhibitors reserpine and GG918 do not inhibit Gram-negative pumps such as MexAB–OprM and this has been explained as being presumably due to differences in cell wall architecture. Looking at the structures of MC-002,595 and MC-207,110, both inhibitors possess lipophilic regions which are probably important for complex formation and transport into the membrane,

and hydrophilic moieties (which are lacking in reserpine and GG918) such as the two primary amine groups. These may be important in facilitating transport of the complex across the hydrophilic domain of the periplasmic space, which is present between the two membranes of Gram-negative bacteria.

At the present time, we cannot correlate the predicted energy of interaction with inhibitory potential due to the fact that the experimental efflux/modulation results come from different in vivo and in vitro studies, and the levels of MDR inhibition were not reported explicitly or were reported using different criteria. We propose three empirical correlations:

1. A low predicted interaction energy (<−9 kcal/mol) results in absence of MDR inhibition.
2. Optimal predicted interaction energy for MDR inhibition is generally greater than −10 kcal/mol. The exception is combinations of taxol and inhibitors (sulindac, tolmetin and indomethacin) where interaction energies were between −9 and −13 kcal/mol, but MDR inhibition was not detected in the experimental studies.²³ However, these interaction energies are lower than interaction energies between other drugs and the same set of MDR inhibitors in that study.²³
3. A high interaction energy between non-drug molecule and inhibitor molecule results in reversal of MDR inhibition.

Our results lead to the conclusion that it is highly likely that inhibitors of MDR have affinity for substrates of efflux transporters, and that they may form complexes which could have a number of roles in the mechanism of MDR inhibition. These complexes may facilitate entry of drugs into the cell and secondly the drug in such a complex may be hidden from MDR transporters. The structural moieties which are present in many MDR inhibitors have been described²⁶ and some of these, notably quinoline and benzyl moieties are found in the drug-binding sites of MDR inhibitors in this study for example GG918 and MC-002,595.

This study may change the perception of MDR inhibition and open further research to find compounds which have good drug-binding capabilities and readily form complexes whilst retaining features which enhance membrane permeability and imperviousness to efflux.

References and notes

1. Ling, V. *Cancer Chemotherapy and Pharmacology* **1997**, 40 (Suppl), S3.
2. Bradley, G.; Ling, V. *Cancer Metastasis Rev.* **1994**, 13, 223.
3. Neyfakh, A. A. *J. Mol. Microbiol. Biotechnol.* **2001**, 3, 151.
4. Neyfakh, A. A. *Molecular Microbiology* **2002**, 44, 1123.
5. Cole, S. P. C.; Bhardwaj, G.; Gerlach, J. H.; Mackie, J. E.; Grant, C. E.; Almquist, K. C.; Stewart, A. J.; Kurz, E. U.; Duncan, A. M. V.; Deeley, R. G. *Science* **1992**, 258, 1650.
6. Ubukata, K.; Itoh-Yamashita, N.; Konno, M. *Antimicrob. Agents Chemother.* **1989**, 33, 1535.

7. Li, X. Z.; Nikaido, H.; Poole, K. *Antimicrob. Agents Chemother.* **1995**, 39, 1948.
8. Ambudkar, S. V.; Dey, S.; Hrycyna, C. A.; Ranmachandra, M.; Pastan, I.; Gottesman, M. M. *Annu. Rev. Pharmacol. Toxicol.* **1999**, 39, 361.
9. Ahmed, M.; Borsch, C. M.; Neyfakh, A. A.; Schuldiner, S. *J. Biol. Chem.* **1993**, 268, 11086.
10. ChemOffice Ultra 2002: CambridgeSoft, 2001.
11. Goodford, P. J. *J. Med. Chem.* **1985**, 28, 849.
12. Schaftenaar, G.; Noordik, J. H. *J. Comput.-Aid. Mol. Des.* **2000**, 14, 123.
13. ViewerLite 5.0, Accelrys Inc, 2002.
14. Bhat, U. G.; Winter, M. A.; Pearce, H. L.; Beck, W. T. *Mol. Pharmacol.* **1995**, 48, 682.
15. de Bruin, M.; Miyake, K.; Litman, T.; Robey, R.; Bates, S. E. *Cancer Lett.* **1999**, 146, 117.
16. Van Rensburg, C. E. J.; Joone, G.; Anderson, R. *Cancer Lett.* **1998**, 127, 107.
17. Gibbons, S.; Oluwatuyi, M.; Kaatz, G. W. *Journal of Antimicrobial Chemotherapy* **2003**, 51, 13.
18. Lomovskaya, O.; Warren, M. S.; Lee, A.; Galazzo, J.; Fronko, R.; Lee, M.; Blais, J.; Cho, D.; Chamberland, S.; Renau, T.; Leger, R.; Hecker, S.; Watkins, S.; Hoshino, K.; Ishida, H.; Lee, V. J. *Antimicrob. Agents Chemother.* **2001**, 45, 105.
19. Chea, X. F.; Nakajimaa, Y.; Sumizawaa, T.; Ikedaa, R.; Rena, X. Q.; Zhenga, C. L.; Mukaia, M.; Furukawaa, T.; Haraguchia, M.; Gaoa, H.; Sugimotob, Y.; Akiyamaa, S. *Cancer Lett.* **2002**, 187, 111.
20. Seiden, M. V.; Swenerton, K. D.; Matulonis, U.; Campos, S.; Rose, P.; Batist, G.; Ette, E.; Garg, V.; Fuller, A.; Harding, M. W.; Charpentier, D. *Gynecologic Oncology* **2002**, 86, 302.
21. Roe, M.; Folkes, A.; Ashworth, P.; Brumwell, J.; Chima, L.; Hunjan, S.; Pretswell, I.; Dangerfield, W.; Ryder, H.; Charlton, P. *Bioorg. Med. Chem. Lett.* **1999**, 9, 595.
22. Choi, C. H.; Sun, K. H.; An, C. S.; Yoo, J. C.; Hahm, K. S.; Lee, I. H.; Sohng, J. K.; Kim, Y. C. *Biochemical and Biophysical Research Communications* **2002**, 295, 832.
23. Duffy, C. P.; Elliott, C. J.; O'Connor, R. A.; Heenan, M. M.; Coyle, S.; Cleary, I. M.; Kavanagh, K.; Verhaegen, S.; O'Loughlin, C. M.; NicAmhlaoibh, R.; Clynes, M. *Eur. J. Cancer* **1998**, 34, 1250.
24. Fua, L. W.; Zhangb, Y. M.; Lianga, Y. J.; Yanga, X. P.; Pana, Q. C. *Eur. J. Cancer* **2002**, 38, 418.
25. Gibbons, S.; Oluwatuyi, M.; Veitch, N. C.; Gray, A. I. *Phytochemistry* **2003**, 62, 83.
26. Klopman, G.; Shi, L. M.; Ramu, A. *Mol. Pharmacol.* **1997**, 52, 323.